Inflammatory state of lymphatic vessels and miRNA profiles associated with relapse in ovarian cancer patients.

Sarah C Johnson[1], Sanjukta Chakraborty[2], Anastasios Drosou[3], Paula Cunnea[4], Dimitrios Tzovara[3], Katherine Nixon [4], David C Zawieja [2], Mariappan Muthuchamy [2], Christina Fotopoulou[4] ¶ and James E Moore jr. [1] ¶ *.

[1] Department of Bioengineering, Imperial College London

[2] College of Medicine, Texas A&M University

[3] Parhelia Analytics

[4] Department of Surgery and Cancer, Imperial College London.

* Corresponding author

Email. james.moore.jr@imperial.ac.uk (JM)

¶ *Christina Fotopoulou and Prof. James E Moore jr. should be considered as joint senior authors.*

Abstract

Lymphogenic spread is associated with poor prognosis in epithelial ovarian cancer (EOC), yet little is known regarding roles of non-peri-tumoural lymphatic vessels (LVs) outside the tumour microenvironment that may impact relapse. We hypothesize that inflammatory status of the LVs and/or changes in the miRNA profile of the LVs, could potentially have a prognostic and predictive value for overall outcome and risk of relapse. Samples of macroscopically normal human lymph LVs (n=10) were isolated from the external iliac vessels draining the pelvic region of patients undergoing debulking surgery. This was followed by quantification of the inflammatory state (low, medium and high) and presence of cancer-infiltration of each LV using immunohistochemistry. LV miRNA expression profiling was also performed, and analysed in the context of high versus low inflammation, and cancer-infiltrated versus non-cancer-infiltrated. Results were correlated with clinical outcome data including relapse with an average follow-up time of 13.3 months**.** The presence of high inflammation correlated significantly with patient relapse ($p=0.033$). Cancer-infiltrated LVs showed a moderate but non-significant association with relapse ($p=0.07$). Differential miRNA profiles were identified in cancer-infiltrated LVs and LVs with high versus low inflammation. In particular, the let-7 family was consistently downregulated < 1.8-fold in highly inflamed LVs ($p<0.05$) as opposed to the less inflamed ones. Down-regulation of the let-7 family appears to be associated with inflammation, but whether inflammation contributes to or is an effect of cancer-infiltration requires further investigation.

Introduction

Epithelial Ovarian cancer (EOC) accounts for over 4000 deaths in the UK every year [1]. Lymph nodes metastases are very common in EOC-patients and also associated with a more dismal overall prognosis [2-3]. Total macroscopic tumour clearance, is one of the most important prognostic factors for survival post-surgery in EOC, including also the removal of bulky lymph nodes [3-4]. There is no therapeutic value in the systematic removal of clinically normal appearing LN in the advanced disease setting, as shown in prospective randomised trials [5]. The involvement and changes in the connecting lymphatic vessels (LVs) and how they are related to the future risk of metastasis and relapse have never been investigated, to our knowledge.

LVs are specialised in the uptake and transport of macromolecules from tissue fluid, consequently permitting lymphogenic spread of cancer cells. Within the tumour microenvironment, intra-tumoural LVs are present, however functional tests in mice have indicated that intra-tumoural lymphatics are non-functional [6,7]. The collapse of intra-tumoural LVs is potentially due to the high interstitial pressure observed in multiple types of tumours, a lack of lymphatic valves, or induced mechanical pressure of growing tumour cells [6]. However, in both mice and humans, functional peri-tumoural lymphatics remain [6]. LVs can facilitate metastases both passively and through active changes in lymphatic endothelial cell (LEC) expression, that aid cancer-cell infiltration, allowing subsequent drainage to LNs [8]. Tumour cells can also arrest within the draining LVs and form in-transit metastases, and in some cases escape the LVs, contributing to loco-regional metastasis, potentially aided by altered LV barrier integrity [8].

70 Lymphatic endothelial cells (LECs) that line the LVs can also modulate immune cell
71 function, in both anti-tumour immune response and cancer-induced immunosuppression [9].
72 For example, LEC expression of Protein-Death-Ligand 1 (PD-L1), the ligand for T cell
73 inhibitory receptor, PD-1, can contribute to peripheral tolerance in LNs and tumours [10].
74 Tumour associated LECs can scavenge and cross-present tumour-antigen to cognate $CD8^+$
75 TCs, displaying the ability to endogenise allergen ovalbumin, then present the exogenous
76 antigen on Major Histocompatibility Complex (MHC) class I molecules, and contribute to
77 inducing tolerance of tumour-specific $CD8^+$ TCS [11]. LECs of the LN can acquire peptide
78 MHCII-from DCs and induce tolerance of $CD4^+$ TCs via subsequent presentation, in addition
79 to up-regulating MHCII in response to viral-induced inflammation or Interferon-gamma
80 (IFN-γ) [12]. The LVs are also sensitive to inflammation-induced signalling molecules which
81 can promote lymphangiogenesis, and induce further secretion of inflammatory molecules that
82 may drain to the LNs [13]. Chronic inflammation in the collecting LVs induce changes
83 including LV dilation and inhibition of contractile ability but the effects on metastasis are
84 unknown [14].
85
86 MicroRNA provide vital post-transcriptional regulation of gene expression, a function that is
87 often disrupted by cancer [15]. The ability of a single miRNA to inhibit multiple target genes
88 has led to several studies of altered tumour miRNA expression in ovarian cancer and
89 response to chemotherapy. This includes comparison of miRNA expression in different
90 tumour subsets, in healthy versus diseased ovaries, in patient versus healthy serum, benign
91 versus malignant tumours, expression associated with reduced patient survival, and
92 expression associated with drug-resistance [16]. For example, a study using both EOC cell
93 lines and EOC tumour tissue showed highly elevated miR-221, decreased miR-21 expression,
94 and down-regulation of several members of the let-7 family [17].

Expression of miRNA in LVs and LECs is altered during inflammation and by nearby tumours. In inflamed LECs, upregulated miR-1236 reduced expression of vascular-endothelial growth factor-3 receptor, inhibiting lymphangiogenesis [18]. A separate study showed that inflamed dermal LECs increased miR-155 expression, a miRNA with known involvement in PD-L1 expression which may contribute to peripheral tolerance changes [19]. Furthermore, a panel of differentially expressed miRNAs was identified in inflamed rat LV and human LEC culture, indicating effects on inflammation, angiogenesis, endothelial mesenchymal transition, cell proliferation and senescence pathways [13]. Tumour expression profiling has identified changes in lymphangiogenesis-inducing miRNAs, such as miR-126 in oral cancer and miR-128 in non-small cell lung cancer, that could influence metastasis [20,21]. A study using human LEC co-culture models of gastric cancer, representing tumoural or draining LVs, identified changes in differential miRNAs expression associated with lymphangiogenesis and with positive lymphatic metastasis [22]. Further miRNA expression studies of draining LVs are lacking but many gene dysregulations were identified in LECs isolated from afferent LVs that drained a metastatic gastric tumour in rats, including up-regulation of chemokine CXCL1 [23].

The aim of this study was to provide insight into the changes in the inflammatory state and miRNA expression of the transporting LVs in EOC. It is expected that these changes will be indicative of the immune response in the LVs and the downstream LN, and therefore could be predictive of patient prognosis.

Methods

LV sample collection

LVs were collected from patients undergoing debulking surgery for advanced stage (FIGO IIC, III or IV) epithelial ovarian cancer at Hammersmith Hospital, Imperial College Healthcare NHS Trust, London, United Kingdom (Tables 1 and S1). Informed consent was provided from each patient. Ethics committee approval was obtained from Hammersmith and Queen Charlotte's and Chelsea Research Ethics Committee (REC reference: 05/Q0406/178), and tissue samples were provided by the Imperial College Healthcare NHS Trust Tissue Bank (ICHTB). The following LV processing steps are summarised in S1 Fig.

Macroscopically normal appearing LVs along the external iliac vessels with surrounding fibro-fatty tissue were removed with the nearby LN as part of the debulking procedure. Vessels were ligated with VIcyl03 or PDS-4-0, avoiding bipolar coagulation and other thermic energy to limit vessel damage. All patients had no macroscopic residual disease after surgery.

141 **Table 1. Summary of the LV microscopic state and clinical data**.

Vessel Sample	Type of marker						
	MPO	WT1	Pax-8	Stage	Histology	LN histology	Relapse*
1	+++	+++	++	IVB	HGS	-	y
2	+++	+++	+++	IVA	HGS	n/a	y
3	+++	-	-	IIC	HGS	n/a	y
4	+	++	+	IV	HGS	n/a	y
5	-	-	-	IIIB	Clear Cell	n/a	n
6	-	-	-	IIIC	HGS	n/a	n
7	-	-	-	IIIC	HGS	+	n
8	-	-	-	IIIC	HGS	n/a	n
9	+	-	-	IVB	HGS	n/a	n
10	+	+	++	IIC	HGS	-	n

Key	MPO	WT1/Pax-8
	+++ high	+>=15 cells
	+ medium	++ 15> cells >=5
	- low	+ < 5 cells

142
143 Sections of the LVs were stained with antibodies for the inflammatory marker
144 myeloperoxidase (MPO), ovarian cancer markers Wilms-Tumour-1 (WT1) and Paired Box
145 Gene 8 (Pax-8), and the lymphatic endothelial marker, Podoplanin (PDPN).
146 *Mean time since surgery = 13.2 ±3.6 months
147

148 **Vessel isolation and storage**

149 Tissue specimens were transported directly from surgical theatre to the laboratory in ice-cold
150 sterile Phosphate Buffered Saline (VWR, UK). LVs were identified and isolated along with a
151 small amount of surrounding tissue under a dissection microscope within a sterile laminar
152 flow cabinet (Fig 1A-C). Each vessel was divided into two sections. One half of each vessel
153 was further cleaned of surrounding fatty tissue, placed in RNA stabilising solution
154 (RNAlater, ThermoFisher, UK), frozen on dry ice and stored at -20°C. The other half was
155 fixed in 4% paraformaldehyde (VWR, UK) for 45 minutes, followed by submersion in 15%

156 sucrose for 3 hours, then 30% sucrose for 6-12 hours. This was followed by embedding in
157 OCT (Scigen, UK) using dry ice and isopropyl alcohol (ThermoFisher, UK) and stored at -
158 80°C.
159
160 **Fig 1. Lymphatic vessel isolation and imaging.** A. LV isolation technique. B. Tissue
161 sample containing LV. C. Isolated and cleaned vessel for RNA extraction. D&E,
162 Quantification of LVs inflammation was determined using the ratio of MPO staining to cell
163 nuclei (DAPI), in this example 1.0%/6.3%= 0.16, to divide samples into low, medium and
164 high inflammatory states with thresholds of <3%, 3-10% and >10% respectively. F. H & E
165 stained sections of the LVs, show that the nuclei were sufficiently preserved for subsequent
166 Paired-Box-Gene 8 (Pax-1) and WT1 (Wilms-Tumour-1) staining. G-I. LVs with no/low,
167 medium and high inflammatory state determined with MPO staining. J. Confirmation of LV
168 status was carried out using LEC marker Podoplanin (PDPN) that stained around the LV
169 lumen. K-L. OC marker WT1 negative/positive LV. N. MPO positive control. O-P. OC
170 marker Pax8 LV negative, LV positive and positive control. M, Q. An Ovarian tumour
171 sample was used as a positive control and stained positively for both WT1 and Pax8.
172 Scale=140µm.
173
174 **MiRNA extraction and analysis**
175 Samples in RNAlater were individually defrosted and homogenized in 700µL of QIAzol
176 (Qiagen, UK), using a PT 1300 D homogenisor with a 3mm dispersing aggregate head
177 (Kinematica, Switzerland) at 20,000 RPM in a sterile 1.5 ml tube. RNA was extracted using a
178 RNeasy Mini Kit (Qiagen, UK) following the standard protocol and quality was verified
179 using a NanoDropTM 2000 at A260/280nm and A260/230nm absorbance (Thermofisher,
180 UK). Each sample was reverse-transcribed to cDNA using a miScript II RT Kit (Qiagen),

181 then qPCR was carried out using a miScriptSybrGreen real-time PCR kit (Qiagen) and pre-
182 defined miScript miRNA PCR Array (Qiagen, UK). The array contained primer pairs for 8
183 housekeeping genes and controls plus 88 human miRNAs that have previously been
184 identified or predicted to target genes involved in the regulation of inflammatory responses
185 and autoimmunity. One well was populated with a negative control sample. The array was
186 run using a StepOnePlus Real-Time PCR System (Applied Biosystems), according to the
187 manufacturer's instructions.
188

189 **Immunofluorescence staining and Imaging**

190 Samples embedded in OCT were sectioned at 10-16μm and stored at -80°C. Both standard
191 Haematoxylin and Eosin (H&E) and immunofluorescent staining were subsequently
192 performed. For immunofluorescent staining, slides were washed with Tris Buffered Saline
193 (TBS) (Sigma-Aldrich, UK) and 0.05% Triton-X (Sigma) and blocked for 1hour with 10%
194 goat serum/TBS (Sigma-Aldrich). Slides were incubated overnight at 4°C with primary
195 antibodies diluted in 5% goat serum/TBS at ratios of 1:200 for inflammatory marker
196 Myeloperoxidase (MPO) (ab9535), 1:200 for ovarian carcinoma marker Wilms Tumour-1
197 (WT1) (ab89901), 1:50 for ovarian carcinoma marker Paired-Box-Gene 8 (Pax-8)
198 (ab189249), and 1:200 for LEC marker Podoplanin (PDPN) (ab10288). Alexa-488
199 conjugated secondary antibody, anti-Mouse (ab150113) or anti-Rabbit (ab150077) were
200 applied at a dilution of 1:250 in 5% goat serum/TBS at room temperature for 1 hour.
201 Samples were stained with DAPI (4',6-diamidino-2-phenylindole) solution (Sigma-Aldrich)
202 and mounted with FluoroshieldTM (Sigma-Aldrich). Confocal Z-stacks and multi-channel
203 images were processed and analysed using FIJI imaging software [24].
204

205 Cryo-sections of LV samples stored at -80°C maintained sufficient morphology to quantify
206 inflammation and cancer cell presence (Fig 1F). The identification of LVs was confirmed by
207 the positive staining with Podoplanin (Fig 1J). The LV were subsequently classified into a
208 low, medium or high inflammatory group with thresholds of <3%, 3-10% and >10% of MPO
209 staining to nuclei (DAPI) staining ratio (Fig 1 D and E). The level of cancer-cell infiltration
210 was determined by the number of cancer cells detected in a LV cross-section, as shown by
211 positive staining with WT1 and Pax-8.
212

213 **Statistical Analysis**

214 Clinical correlation between different combinations of LV state (inflammation, high-
215 inflammation, cancer-infiltration), and patient relapse, and cancer-stage were assessed by
216 applying Fishers exact test, to identify significant non-random associations, and calculation
217 of Cohen's Kappa coefficient of inner agreement (κ), interpreted according to the methods of
218 Vierra and Garett 2005 [25]. A P value below 0.05 was considered statistically significant
219 and indicated with asterisk: *P < 0.05, **P < 0.01, ***P < 0.001.
220 Prior to further analysis, the miRNA expression of each LV (ΔCT) was normalized to the
221 expression of a stably expressed gene in each array, confirmed with NormFinder
222 (http://moma.dk/normfinder-software) and GeNorm (http://www.biogazelle.com/qbaseplus)
223 software. SNORD96 was selected, due to prior designation, as a housekeeping gene. The fold
224 change between imaging-informed groups of LVs was calculated as ΔΔCT Group2/ΔΔCT
225 Group1 where ΔΔCT=2^{Δ}CT. Fold regulation was normalised to values greater than 1, noting
226 up- or down-regulation. A principle component analysis (PCA) was applied to separate
227 samples based on miRNA expression across two principle components (PC) that account for
228 the greatest sources of miRNA variation within samples, using online software ClustVis
229 (https://biit.cs.ut.ee/clustvis/) [26]. Pathway analysis of the up-regulated and down-regulated

genes identified was carried out using Diana-MiRPath v3 [27]. A student-t-test, assuming equal variance, was applied to further confirm variation between groups. To visualise the distributions of the individual miRNA for which statistical significant difference was identified between groups, the probability density functions for miRNA expression in each group were estimated using Kernel Density Estimated distributions.

Supervised learning classification algorithms were then implemented to classify the samples' states into groups (inflamed/cancer-infiltrated/relapsed/stageIV) based on miRNA expression. The methods used were Logistic Regression Model, k-Nearest Neighbours, Support Vector Machine, Random Forest Classifier and Gaussian Naïve Bayes (See supplement for further details). Training of models was achieved using Leave One Out Cross Validation with accuracy defined as the percentage of correct classifications. A McNemar's test of homogeneity of the predicted probabilities between the inner groups was applied and Cohen's Kappa coefficient (κ) calculated between predicted and actual results. The ability of a miRNA to be distinguished between groups, was identified using a t-test. A set of only the miRNA that were significantly differentially expressed between groups was then used to train new classifiers. Whether use of the new classifier could improve predictions was then assessed, compared to performance of classifiers built using the entire miRNA expression set.

Data availability

Further analytical results are available in the supplementary material. All raw and normalised expression data files are available from the [tbc] database (accession number(s) [tbc], [tbc].).

Results

Post-operative assessment of patients

Ten patients were included in the present analysis. Nine of those patients had a high grade serous histology, and one patient had a clear cell carcinoma (Table 1). 60% of the lymph vessels were harvested at primary debulking surgery and 40% at interval debulking surgery (S1 Table). Only one positive para-aortic LN was detected at final histopathology. In the 13.2±3.6 months follow up period, 4 of the 10 patients had relapsed. Of the four patients that relapsed, three vessels demonstrated high inflammation and one vessel showed medium inflammation. Vessels from patients that did not relapse showed low inflammation in 4 cases and medium inflammation in the remaining 2 cases. Of the four relapse cases, cancer-cell infiltration was detected in three vessels (two with high inflammation and one showing medium inflammation).

Clinical correlation of LV inflammatory state or cancer-cell infiltration and patient relapse

Of the four cancer-infiltrated LVs identified, 2 presented with high inflammation and the remaining 2 samples presented with medium inflammation. Cancer-free LVs presented with generally lower degrees of inflammation (Table 1). Tumour cells were detected in 50% of LVs with medium inflammation and two-thirds of LVs displaying high inflammation. The LVs presented with high inflammation in 3 of 10 samples, two of which were also positive for cancer cells**.** Three LV samples presented with medium inflammation, two of which contained cancer cells, and the remaining 4 LV samples presented with low inflammation and no detectable cancer cell infiltration (Table 1). The samples were macroscopically normal in appearance, however positive staining for the ovarian tumour markers WT1 and Pax8 was

observed in four of the 10 samples collected (Fig 1 L,P). The LVs with cancer cells showed a moderate agreement (κ=0.583) with patient relapse but this was not significant (Table 2) (p=0.114). A moderate but statistically non-significant agreement was found between cancer-infiltrated LVs and Stage IV and inflammation (κ =0.583, 0.61 respectively).

Table 2: Cohen's Kappa Coefficient for inner-agreement between different sample states (1=perfect agreement) and Fisher's exact test for identification of significant non-random association (p<0.05) (n=10).

Cohen's Kappa Co-efficient					
	Relapse*	**Inflam.**	**High Inflam.**	**Cancer-cell inf.**	**Stage IV**
Relapse	x	**0.615**	**0.783**	0.583	0.583
Inflam.	**0.615**	x	x	**0.615**	**0.615**
High Inflam.	**0.783**	x	x	0.348	0.348
Cancer-cell inf.	0.583	**0.615**	0.348	x	0.583
Stage IV	0.583	**0.615**	0.348	0.583	x

Fishers Exact Test (p-value)					
	Relapse*	**Inflam.**	**High Inflam.**	**Cancer-cell inf.**	**Stage IV**
Relapse	x	**0.071**	**0.033**	0.114	0.114
Inflam.	**0.071**	x	x	**0.071**	**0.071**
High Inflam.	**0.033**	x	x	0.300	0.300
Cancer-cell inf.	0.114	**0.071**	0.300	x	**0.114**
Stage IV	0.114	**0.071**	0.300	0.114	x

Inflam = comparison of LVs with high or medium inflammation to low inflammation. High Inflam. = comparison of LVs with high inflammation to low or medium inflammation. Cancer-cell inf. = cancer-cell infiltration.

** Mean time since surgery= 13.2 months ±3.6*

292 As the degree of inflammation in the LVs increased, so did correlation with patient relapse.
293 The presence of LVs showing high inflammation significantly correlated with patient relapse
294 (κ= 0.783, p=0.03) (Table 3). The presence of medium or high inflammation within LVs
295 showed a moderate agreement with patient relapse (κ= 0.615, p=0.07) and patients with Stage
296 IV, relapse and cancer-cell infiltration (κ=0.615, p=0.07) (Table 2). Omitting the LVs with
297 medium inflammation resulted in a stronger correlation involving high inflammation status.
298 LVs exhibiting high degrees of inflammation showed near perfect agreement with patient
299 relapse compared to those with low inflammatory state (n=7, κ=1.0, p = 0.029). Additionally,
300 there were indications of a relationship between highly inflamed vessels with cancer-
301 infiltration and Stage IV cancer (κ=0.695), but this lacked statistical significance (p=0.143).
302 These results therefore support the earlier identified correlation between high inflammation
303 and relapse. Of note, the low, medium and high inflammatory state of the LVs was
304 determined based on relative thresholds amongst the vessels, but all vessels showed less
305 inflammation than similarly stained ovarian tumour tissue (Fig 1N).
306
307 **Table 3: Assessment of Cohen\s Kappa Coefficient and Fisher's exact test, as described**
308 **in Table 2, comparing LVs with high inflammation to LVs with low inflammation only**
309 **(n-7).**

	Relapse	**Cancer**	**Stage IV**
Cohen's Kappa Co-efficient	**1**	0.695	0.695
Fishers Exact Test	**0.029**	0.143	0.143

310
311

312 **Lymphatic Vessel miRNA expression during EOC**

313 Expression analysis of a panel of miRNA involved in auto-immunity and inflammation was
314 carried out. This showed that let-7 was differentially expressed in the highly-inflamed LVs.
315 Significant differential expression of 8 miRNA was identified when comparing miRNA
316 expression of LVs presenting with high inflammation versus low inflammation ($p<0.05$,
317 n=7). Of the 8 miRNA, 6 belonged to the let-7 family with miR-23a-3p and miR-23b-3p
318 completing the set. During analysis, equal variance of each group was assumed, which was
319 supported by the results of analyses of unequal variance (Welches test) and Levene's test
320 under a significance test of 0.05 (S4 Table**).** Differential expression can also be clearly
321 visualised when the estimated probability density functions, calculated using kernel density
322 estimation for inner groups, for the differentially expressed individual miRNA are compared
323 (S2 Fig).

324

325 An overlap was observed between the differential miRNA expression identified in cancer-
326 cell-infiltrated and inflamed LVs and the differential miRNA expression in LVs collected
327 from patients who underwent relapse post-surgery during the study. Four significantly
328 differentially expressed miRNA were identified in relapse LVs (let-7c-5p, let-7b-5p, miR-
329 23b-3p and miR-186-5p), with three of these (let-7c-5p, let-7b-5p, miR-186-5p), also
330 significantly differentially expressed in inflamed and cancer-infiltrated LVs (Fig 2, S2 & S4
331 Tables). Of the 15 miRNA that were down-regulated >1.8 fold in relapse vessels, 13 were
332 also down-regulated in inflamed LVs, including 6 members of the let-7 family and miR-23a-
333 3p and miR-23b-3p.

334

335 **Fig 2: The overlap in differential expression of miRNA in inflamed, cancer-infiltrated**
336 **and relapse-associated LVs.** The (a) up-regulated and (b) down-regulated miRNA identified

337 in three separate comparisons. In the first group cancer-infiltrated LVs were compared to
338 non-cancer-infiltrated LVs. In the second group LVs presenting with high inflammation were
339 compared to those with low inflammation. In the 3rd group miRNA expression in LVs from
340 patients who relapsed during the study duration was compared to miRNA expression in LVs
341 from those who did not relapse.
342
343 In the cancer-infiltrated LVs, most miRNA expression changes involved miRNA up-
344 regulation such as miR-16-5p, miR-93-5p and miR-497-5p, miR-381-3p, miR-144-3p and
345 miR-181a-5p. In contrast, inflamed LVs presented with primarily down-regulated miRNA, in
346 particular, significant down-regulation of members of the let-7 family along with miR-23a-
347 3p, miR-23b-3p and tumour suppressor miR-15-5p [28]. In cancer-containing LVs, 70% of
348 the miRNA that were down-regulated >1.8 fold were also down-regulated in the LVs of
349 patients who relapsed post-surgery during the study period and the inflamed LVs, of which
350 all were members of the let-7 family.
351
352 An overlap in the differential miRNA expression in cancer-infiltrated LVs and inflamed LVs
353 was identified, as 18 miRNA were found to undergo an expression change of >1.8 fold (up-
354 or down-regulated) in both of the comparisons (Table 4, Fig 2). 6 of the 7 miRNA that were
355 down-regulated in both groups belonged to the let-7 family. Of the miRNA that showed
356 increased expression, miR-381-3p, miR-93-5p, miR-144-3p and miR-497-5p showed
357 significant differential expression in both inflamed and cancer-infiltrated LVs. The overlap in
358 fold-change difference in the inflamed and cancer-infiltrated LVs may be reflective of the
359 fact that 50% of the cancer-infiltrated LVs also presented with high inflammation. More
360 significant differences were identified between vessels with high or low inflammation than

361 vessels with or without cancer-infiltration. Expression of several miRNA were consistently

362 not detected by qPCR and omitted from further analysis.

363

364 **Table 4: Differential expression of miRNA between LV groups.**

Inflamed compared to Non-Inflamed			Cancerous compared to Non-Cancerous		
miRNA	**Fold Regulation**	**p value**	**miRNA**	**Fold Regulation**	**p value**
miR-301a-3p	13.657	0.34	**miR-144-3p**	**14.02**	**0.001**
miR-186-5p	6.327	0.104	**miR-181c-5p**	**10.629**	**0.017**
miR-410-3p	5.817	0.167	miR-301a-3p	7.3	0.309
miR-19a-3p	5.74	0.385	miR-19a-3p	6.896	0.197
miR-144-3p	4.933	0.193	miR-19b-3p	6.055	0.147
miR-19b-3p	4.423	0.343	miR-101-3p	5.083	0.074
miR-101-3p	4.18	0.34	**miR-381-3p**	**4.07**	**0.014**
miR-29b-3p	2.528	0.348	miR-181a-5p	3.875	0.274
miR-590-5p	2.453	0.792	miR-130a-3p	3.853	0.115
miR-497-5p	2.442	0.289	miR-186-5p	3.214	0.131
miR-15a-5p	2.301	0.405	let-7a-5p	2.92	0.287
miR-381-3p	2.175	0.24	**miR-497-5p**	**2.902**	**0.026**
miR-195-5p	-1.945	0.132	miR-590-5p	2.78	0.521
miR-29a-3p	-2.013	0.724	miR-15a-5p	2.767	0.182
let-7i-5p	-2.132	0.078	**miR-93-5p**	**2.252**	**0.001**
miR-301b-3p	-2.605	0.43	miR-29a-3p	2.166	0.525
miR-23a-3p	**-2.889**	**0.018**	miR-29b-3p	2.098	0.32
let-7g-5p	-3.122	0.121	**miR-16-5p**	**2.077**	**0.031**
let-7e-5p	**-3.163**	**0.04**	**let-7i-5p**	**-2.08**	**0.021**
let-7f-5p	**-3.462**	**0.041**	let-7b-5p	-2.274	0.07
miR-98-5p	-3.79	0.168	let-7e-5p	-2.505	0.432
miR-15b-5p	**-4.167**	**0.047**	let-7c-5p	-2.556	0.078
let-7d-5p	**-4.907**	**0.004**	let-7d-5p	-2.672	0.122
miR-202-3p	-5.95	0.236	let-7f-5p	-3.239	0.27
miR-181d-5p	-6.426	0.131	miR-202-3p	-4.8	0.299
let-7c-5p	**-6.666**	**0.001**			
miR-130a-3p	-6.752	0.652			
let-7b-5p	**-11.026**	**0.003**			
miR-23b-3p	**-13.016**	**0.01**			
let-7a-5p	**-222.405**	**0.024**			

up-regulated | down-regulated | **Bold= p < 0.05**

365

366 Listed are miRNA that showed a fold-change ±1.8 and/ or a significant difference between

367 groups (t-test p>0.05)

368

369 **Pathway Analysis of miRNA found to be dysregulated in inflamed or cancer-**

370 **infiltrated LVs**

371 Pathway analysis indicated that significantly dysregulated miRNAs are involved in

372 maintaining LV integrity. The miRNA that were significantly upregulated in cancer-

373 infiltrated LVs, and those significantly down-regulated in inflamed LVs have known

374 involvement in various pathways related to the TGFβ-pathway, fatty acid biosynthesis,

375 proteoglycans in cancer, glycosaminoglycan synthesis and glycan biosynthesis as well as the

376 extracellular matrix receptor interactions pathway and adherens junction pathway (Table 5).

377

378

379

380

381

382

383

384

385

386

387

388

389

390

391

392

393 **Table 5: Pathway analysis using miRNA.**

Upregulated miRNA				Down-regulated miRNA			
KEGG pathway	p-value	Genes	miRNA	KEGG pathway	p-value	Genes	miRNA
TARBASE							
Proteoglycans in cancer	3.02E-15	96	5	Adherens junction	5.86E-13	52	8
Adherens junction	3.09E-09	44	5	Proteoglycans in cancer	5.86E-13	107	8
Prion diseases	3.09E-09	14	5	TGF-β signaling pathway	3.29E-09	49	8
Viral carcinogenesis	1.64E-08	91	5	Viral carcinogenesis	5.77E-09	99	8
Hippo-signaling pathway	2.37E-08	68	5	Cell cycle	2.79E-08	74	8
TGF-β signaling pathway	9.56E-08	41	5	Hippo signaling pathway	1.24E-07	74	8
TARGETSCAN							
Fatty acid biosynthesis	7.90E-38	2	2	Fatty acid biosynthesis	2.92E-53	3	1
Fatty acid metabolism	8.15E-15	3	2	Fatty acid metabolism	1.03E-21	4	1
Metabolism of xenobiotics by cytochrome P450	7.48E-06	2	2	Signaling pathways regulating pluripotency of stem cells	2.58E-09	17	7
Signaling pathways regulating pluripotency of stem cells	6.26E-05	11	3	Metabolism of xenobiotics by cytochrome P450	8.99E-07	3	3
TGF-β signaling pathway	0.0387	5	3	N-Glycan biosynthesis	0.00466	5	3
Micro-CT-DS							
Fatty acid biosynthesis	7.90E-38	5	2	Fatty acid biosynthesis	7.39E-26	6	9
Fatty acid metabolism	8.15E-15	11	2	ECM-receptor interaction	3.21E-07	17	9
Signaling pathways regulating pluripotency of stem cells	3.74E-12	47	3	Signaling pathways regulating pluripotency of stem cells	1.01E-06	43	9
Hippo signaling pathway	2.06E-06	29	2	Mucin type O-Glycan biosynthesis	5.38E-06	9	9
Proteoglycans in cancer	2.70E-06	59	4	Proteoglycans in cancer	2.34E-05	53	9
				p53 signaling pathway	3.13E-05	27	9

394 MiRNA that were significantly up-regulated in cancer-infiltrated LVs (left-hand side) and

395 miRNA significantly down-regulated >1.8 fold (right-hand side) in highly inflamed LVs.

396

397 **Principle component analysis of miRNA expression in LV samples.**

398 The use of principle component analysis showed that differential miRNA expression

399 identified in inflamed and cancer-infiltrated LVs could also be identified without grouping

400 the samples. This can be seen when assessing the top 16 miRNA whose expression

401 contributed the most principle components, PC1 and PC2, that account for the most variation
402 between samples (S3 Fig). Twelve miRNA identified in the fold-change analysis of highly
403 inflamed or cancer-infiltrated LVs, were among the top 20 miRNA that contributed to PC1,
404 with 5 of those showing significant differential expression. Furthermore, 8 miRNAs of the
405 top 20 miRNA that contributed to PC2 were all identified as significantly downregulated
406 >1.8 fold in highly inflamed LVs. The remaining miRNA varied greatly between the patient
407 samples, e.g., miR-20, but were not identified by analysis of fold change between groups.
408 The expression levels of these miRNA were therefore spread equally between the compared
409 groups. Overall, variation over PC2 differentiates between highly-inflamed and non-inflamed
410 LVs, supporting the suggestion that miRNA expression could distinguish LV states (S3 Fig).
411

412 **Application of machine-learning algorithms to predict LV state or clinical**
413 **outcome based on miRNA expression**

414 Patterns of miRNA expression showed some potential in predicting clinical outcomes by
415 applying classification algorithms. When predicting patient relapse, all of the classification
416 methods presented with quite high accuracy values and McNemar's probabilities of $p<0.05$,
417 meaning that no significant difference was found between the predicted grouping, based on
418 miRNA expression, and the grouping based on the known clinical data. Of the methods
419 applied, use of k-Nearest Neighbours and logistic regression produced the best classification
420 with similar prediction accuracy achieved between methods (Table 6). Classification of
421 cancer-cell infiltrated LVs based on miRNA expression showed a similar prediction accuracy
422 compared to classification of relapse LVs, but the Random Forest classifier achieved the best
423 accuracy (Table 7). Classification of inflamed and <=Stage IV samples did not show a good
424 accuracy (S3 Table). The effects of significantly differentially expressed miRNAs ($p<0.05$)
425 between groups were further assessed by building classifiers using only significant miRNA.

426 Prediction of relapse based on miR-23b-3p and miR-186-5p expression, improved the
427 accuracy of classification with all classification methods by 10% except when using Support
428 Vector Machines, where no improvement was observed (see S5 Table & S1 File). Addition
429 of miR-let-7b-5p and let-7c-5p improved the accuracy of Support Vector Machines from
430 80% to 90% but decreased the accuracy of logistic regression from 80% to 70%. However,
431 use of miR-23b and miR-186-5p only showed a bias towards classifying the samples as non-
432 relapsed when using Logistic Regression which decreased when using all 4 miRNA.
433
434 **Table 6: Classification analysis performance for various supervised classification**
435 **algorithms predicting patient relapse based on LV miRNA expression.** Displays the
436 accuracy of the algorithm, Cohen's Kappa of inner agreement between predicted and actual
437 values and the accuracy for inner groups during the relapse case. Also, there is McNemar's
438 test significance of equality of predicted probability (inner accuracy) between groups for each
439 state.

Method	Accuracy	McNemar's Test-pval	Cohen's Kappa	No Relapse	Yes Relapse
Logistic Regression	70%	0.999	0.375	67.0%	75.0%
K-Nearest Neighbours	80%	0.289	0.583	100.0%	50.0%
Support Vector Machines	80%	0.289	0.583	100.0%	50.0%
Random Forests Classifier	50%	0.375	-0.042	67.0%	25.0%
Gaussian Naive Bayes	60%	0.031	0.167	100.0%	0.0%

440
441
442
443

444 **Table 7: The classification accuracy when building classifiers (as described above) to**

445 **predict cancer-infiltration based on the LV miRNA expression.**

Method	Cancer-cell infiltration				
	Accuracy	McNemar's Test-pval	Cohen's Kappa	No Cancer	Yes Cancer
Logistic Regression	70%	0.44	0.374	83.3%	50.0%
K-Nearest Neighbours	50%	0.37	-0.04	67.0%	25.0%
Support Vector Machines	70%	0.13	0.37	100.0%	25.0%
Random Forests Classifier	100%	1	1	100.0%	100.0%
Gaussian Naive Bayes	50%	0.37	-0.04	67.0%	25.0%

446

447 # Discussion

448 To our knowledge, this is the first analysis of inflammatory and miRNA alterations in tumour
449 draining LVs in ovarian cancer. We aimed to provide insights into LV features that might be
450 associated with patient relapse. Our results may contribute to a better prediction of patient
451 relapse, and could guide future experimental work seeking to improve patient outcome via
452 therapeutic targeting of miRNA.

453

454 Macroscopically normal LVs, remote from the tumour site that exhibited high or medium
455 inflammation correlated with cancer relapse. Despite cancer-cell infiltration in 66% of these
456 vessels, a moderate but non-significant association was identified between inflamed and
457 cancer-infiltrated LVs (p=0.07). The staging of LNs is routinely used to quantify cancer
458 progression but the status of the connecting LVs has not previously been investigated. While
459 case numbers are small, the presence of high inflammation in the LVs showed the strongest
460 significant correlation with cancer relapse (p=0.03 **κ**=0.783). Whether inflammation is a

461 consequence of factors that contribute to relapse, or the inflammation-induced changes
462 directly affect relapse, is an area for future work.
463
464 Analysis of the effect of cancer cell infiltration of the LVs, without considering LV
465 inflammatory state, identified a trend towards a non-significant association with relapse
466 (p=0.07, **κ**=0.783). This suggests that cancer-infiltration of LVs alone may not necessarily
467 predict relapse, but rather accompanying changes in vessel inflammation may increase the
468 likelihood of relapse. Furthermore, cancer-cell infiltration did not show a significant
469 association with high inflammation. The lack of a significant correlation in both cases may
470 also be simply due to the possible scenario that cancer cells are just transiting through these
471 vessels, so detecting their presence becomes a matter of timing. Overall, this study suggests
472 that nearby LVs appear to play an important role in the immune response to cancer and the
473 association between inflammatory lymphatic changes and relapse deserves further
474 exploration while potentially representing a therapeutic target.
475
476 The use of miRNA expression classification algorithms also showed potential to predict
477 relapse, with relatively high accuracy for these 10 patients when applying a k-Nearest
478 Neighbours algorithm or a Support Vector Machine model (80%) (Table 6, S5). Further
479 studies spanning a larger number of patients should therefore be performed. Clinically, the
480 prediction of a patient's outcome based on miRNA expression of tissue collected during
481 surgery could be of considerable value. Assessment of individual miRNAs showed that in
482 cancer-infiltrated LVs, the differentially expressed miRNAs enhanced the accuracy of the
483 predictive algorithm, reaching 80-100% accuracy (S5 Table). Prediction of relapse was also
484 improved in four of the five classification methods, reaching a maximum of 90% accuracy,
485 when using expression of the significantly differentially expressed miRNA only (let-7b-5pk,

486 let-7c-5p, miR-23b-3p and miR-186-5p). However, despite the presence of inflammation
487 showing a moderate agreement with relapse and high inflammation displaying a significant
488 correlation with relapse, a classifier based on miRNA expression in high or medium inflamed
489 LVs did not show a high accuracy (Tables 2 & 3, S3 & S5 Table). Furthermore, due to the
490 limited number of highly inflamed LVs, it was not possible to build a reliable classifier based
491 on miRNA expression in LVs with high inflammation versus miRNA expression in LVs with
492 low or medium inflammation. Indeed, all the classifiers are limited by the number of samples
493 required to train the predictive algorithms. Therefore, whilst providing insight, these
494 observations require increased sample input to maintain confidence in miRNA classification.
495
496 Analysis of miRNA expression of highly inflamed LVs compared to LVs with no or low
497 inflammation, showed down-regulation of 6 members of the let-7 family. The change in let-7
498 miRNA expression was large enough that without designating groups, the overall variability
499 in sample miRNA expression due to let-7 expression could be detected using PCA (S3 Fig).
500 In ovarian tumour tissue, let-7 expression is down-regulated and associated with poor
501 prognosis and chemo-resistance [17,29,30]. Let-7 family members target oncogenes HMAG2
502 and RAS, and loss of let-7 is also associated with the development of aggressive cancers [31].
503 Chemo-sensitivity of tumours may also be affected by let-7 expression. Manipulation of let-
504 7e in EOC cells *in-vitro* and *in-vivo* confirmed that expression is reduced in cisplatin-resistant
505 cell lines and application of let-7e mimics alongside cisplatin, reduced tumour growth in
506 mice more than with cisplatin alone [32]. Furthermore, chimeric-mediated delivery of let-7i
507 miRNA to EOC cells *in-vitro* reversed paclitaxel-induced chemo-resistance [33]. Expression
508 of let-7 is also associated with control of the Cdk-dependent cell cycle network, that drives
509 the cell transformation network, allowing cells to undergo an epigenetic switch between non-
510 transformed and a malignant transformed state [34].

511

512 The implications of let-7 downregulation in LVs include changes in immune response and
513 LV permeability. Members of the let-7 family can target inflammatory cytokines, such as IL-
514 6 by let-7a and IL-13 by let-7f, shown to contribute to cancer-cell apoptosis and anti-
515 inflammatory action respectively [35,36]. In addition to affecting immune cells in transit,
516 drainage of cytokines to LNs could impact immune response at the LN, potentially
517 contributing to the loss of immuno-suppression observed in draining LNs [37]. Cytokines
518 may also affect LV transport, as IL-6 can increase LV permeability while intradermal
519 administration of cytokines IL-1β, TNF-α, and IL-6 have been shown to decrease lymphatic
520 pulsing frequency [38,39]. Down-regulation of let-7 in vascular endothelial cells is
521 associated with increased TGF-β signalling leading to promotion of epithelial-to-
522 mesenchymal transition and thus increased vessel permeability, but the effects in LVs are
523 currently unknown [40]. The observed up-regulation of several miRNA (miR-381-3p, miR-
524 15a-5p, miR-93-5p, miR-16-5p and miR-497-5p) in cancer-infiltrated LVs may inhibit
525 Vascular Endothelial Growth Factor (VEGF) expression or VEGF receptors, both directly
526 and indirectly via Bcl-2 inhibition [41-44]. The inhibition of VEGF secretion in tumours has
527 been a target of several drug trials but manipulation of VEGF secretion in connecting LVs
528 may present as a future therapeutic area [45]. Expression of miR-181a-5p is also known to
529 regulate the expression of PROX-1 in LECs, a gene whose expression is required to maintain
530 LEC phenotypes [46,47].

531

532 The pathway analysis of the dysregulated miRNA identified involvement in transforming-
533 growth factor TGF-β2 signalling, as well as glycoproteins in cancer and molecules that
534 contribute to the glycocalyx of the LV lumen (Table 5). LECs present with a thick glycocalx
535 composed of glycoprotein side chains, a backbone that includes adhesion molecules, and a

536 proteoglycan core. Therefore, changes to glycoproteins or adherens junctions may affect
537 integrity of the LV wall [48]. Furthermore, a study by Zolla *et al* showed aged collecting LVs
538 in rats presented with a thinner endothelial cell glycocalyx and a loss of gap junction proteins
539 [49]. Functionally this resulted in hyper-permeability of the LVs that allowed pathogens to
540 escape into surrounding tissue. This may suggest that the miRNA changes that accompany
541 cancer cell infiltration and inflammation may also alter LV permeability and barrier function.
542 This in turn could aid cancer cell infiltration but may also impact similar movements of
543 immune cells such as macrophages and dendritic cells [50]. Further studies to assess the
544 impact of inflammation-induced miRNA expression changes on LV integrity may identify
545 new avenues to prevent transmigration of cancer cells across LV walls.
546
547 A notable limitation to this study is the lack of samples from healthy controls. However, this
548 means that the changes in LV status are directly relevant to identification of factors that aid
549 prognosis, rather than identifying systemic EOC changes compared to healthy subjects.
550 Although our results support a link between systemic inflammation and cancer cell
551 dissemination, a larger study is warranted to validate our findings and also allow further
552 analysis to better identify miRNA patterns using predictive algorithms with greater
553 confidence.

554 # Conclusions

555 In conclusion, we have demonstrated that LVs appear to show quantifiable inflammatory and
556 infiltrative alterations in patients with advanced EOC and that a high inflammatory LV state
557 significantly correlates with higher risk of post-surgical relapse. Macroscopically normal
558 lymphatic LVs show accompanying alterations in miRNA expression that may impact LV
559 integrity and secretion of VEGF and inflammatory cytokines. Whether LV inflammation is a

560 cause or consequence of cancer-cell infiltration is yet to be determined, but our results
561 suggest systemic inflammation as a new area to target.

562 Acknowledgements

563 Tissue samples were provided by the Imperial College Healthcare NHS Trust Tissue Bank.
564 Other investigators may have received samples from these same tissues. The research was
565 supported by the Experimental Cancer Medicine Centre (ECMC, Hammersmith Campus) and
566 National Institute for Health Research (NIHR) Biomedical Research Centre based at Imperial
567 College Healthcare NHS Trust and Imperial College London. The views expressed are those
568 of the author(s) and not necessarily those of the NHS, the NIHR or the Department of Health.

569 References

570 1. UK CR. Cancer Research UK. 2018. Available from:
571 https://www.cancerresearchuk.org/health-professional/cancer-statistics/statistics- by-
572 cancer-type/ovarian-cancer.
573 2. Bachmann C, Bachmann R, Kraemer B, Brucker SY, Staebler A, Fend F, et al.
574 Prevalence and distribution pattern of nodal metastases in advanced ovarian cancer.
575 Molecular and Clinical Oncology. 2016;5(4):483–487.
576 3. Bachmann C, Bachmann R, Fend F, Wallwiener D. Incidence and Impact of Lymph
577 Node Metastases in Advanced Ovarian Cancer: Implications for Surgical Treatment.
578 Journal of Cancer. 2016;7(15):2241–2246.
579 4. Wimberger P, Lehmann N, Kimmig R, Burges A, Meier W, Bois AD. Prognostic
580 factors for complete debulking in advanced ovarian cancer and its impact on survival.
581 An exploratory analysis of a prospectively randomized phase III study of the

582 Arbeitsgemeinschaft Gynäekologische Onkologie Ovarian Cancer Study Group
583 (AGO-OVAR). Gynecologic Oncology. 2007;106(1):69 - 74.
584 5. Harter P, Sehouli J, Lorusso D, Reuss A, Vergote I, Marth C, et al. A Randomized
585 Trial of Lymphadenectomy in Patients with Advanced Ovarian Neoplasms. N Engl
586 J Med. 2019;380(9):822-832
587 6. Padera TP, Kadambi A, Tomaso E, Carreira CM, Brown EB, Boucher Y, et al.
588 Lymphatic Metastasis in the Absence of Functional Intratumor Lymphatics. Science.
589 2002;296(5574):1883–1886.
590 7. Leu AJ, Berk DA, Lymboussaki A, Alitalo K, Jain RK. Absence of Functional
591 Lymphatics within a Murine Sarcoma: A Molecular and Functional Evaluation.
592 Cancer Research. 2000;60(16):4324–4327.
593 8. Jones D, Pereira ER, Padera TP. Growth and Immune Evasion of Lymph Node
594 Metastasis. Frontiers in oncology. 2018;8:36;36–36.
595 9. Stachura J, Wachowska M, Kilarski WW, Güc E, Golab J, Muchowicz A. The dual
596 role of tumor lymphatic vessels in dissemination of metastases and immune response
597 development. Oncoimmunology. 2016;5(7): e1182278.
598 10. Dieterich LC, Ikenberg K, Cetintas T, Kapaklikaya K, Hutmacher C, Detmar M.
599 Tumor- Associated Lymphatic Vessels Upregulate PDL1 to Inhibit T-Cell Activation.
600 Frontiers in immunology. 2017;8:66.
601 11. Lund A, Duraes F, Hirosue S, Raghavan V, Nembrini C, Thomas S, et al. VEGF-C
602 Promotes Immune Tolerance in B16 Melanomas and Cross-Presentation of Tumor
603 Antigen by Lymph Node Lymphatics. Cell Reports. 2012;1(3):191-199.
604 12. Dubrot J, Duraes FV, Potin L, Capotosti F, Brighouse D, Suter T, et al. Lymph node
605 stromal cells acquire peptide–MHCII complexes from dendritic cells and induce

606 antigen-specific CD4+ T cell tolerance. Journal of Experimental Medicine.
607 2014;211(6):1153–1166.
608 13. Chakraborty S, Zawieja DC, Davis MJ, Muthuchamy M. MicroRNA signature of
609 inflamed lymphatic endothelium and role of miR-9 in lymphangiogenesis and
610 inflammation. American Journal of Physiology - Cell Physiology.
611 2015;309(10):C680–C692.
612 14. Liao S, Cheng G, Conner DA, Huang Y, Kucherlapati, RS, Munn, LL, et al. Impaired
613 lymphatic contraction associated with immunosuppression. Proceedings of the
614 National Academy of Sciences of the United States of America. 2011;108(46):18784–
615 18789.
616 15. Calin GA, Croce CM. MicroRNA signatures in human cancers. Nature Reviews
617 Cancer. 2006;6: 857-866.
618 16. Deb B, Uddin A, Chakraborty S. miRNAs and ovarian cancer: An overview. Journal
619 of Cellular Physiology. 2018;233(5):3846-3854.
620 17. Dahiya N, Sherman-Baust CA, Wang TL, Davidson B, Shih I, Zhang Y, et al.
621 MicroRNA Expression and Identification of Putative miRNA Targets in Ovarian
622 Cancer. PLOS ONE. 2008;3(6):1-11.
623 18. Jones D, Li Y, He Y, Xu Z, Chen H, Min W. Mirtron MicroRNA-1236 Inhibits
624 VEGFR- 3 Signaling during Inflammatory Lymphangiogenesis. Arteriosclerosis,
625 Thrombosis, and Vascular Biology. 2012;32(3):633–642.
626 19. Yee D, Shah KM, Coles MC, Sharp TV, Lagos D. MicroRNA-155 induction via
627 TNF- and IFN-suppresses expression of programmed death ligand-1 (PD-L1) in
628 human primary cells. The Journal of Biological Chemistry. 2017;292(50):20683–
629 20693.

630 20. Sasahira T, Kurihara M, Bhawal UK, Ueda N, Shimomoto T, Yamamoto K, et al.
631 Downregulation of miR-126 induces angiogenesis and lymphangiogenesis by
632 activation of VEGF-A in oral cancer. British Journal of Cancer. 2012;107:700-706.
633 21. Hu J, Cheng Y, Li Y, Jin Z, Pan Y, Liu G, et al. microRNA-128 plays a critical role in
634 human non-small cell lung cancer tumourigenesis, angiogenesis and
635 lymphangiogenesis by directly targeting vascular endothelial growth factor-C.
636 European Journal of Cancer. 2014;50(13):2336-2350.
637 22. Yang B, Jing C, Wang J, Guo X, Chen Y, Xu R, et al. Identification of microRNAs
638 associated with lymphangiogenesis in human gastric cancer. 2013;16.
639 23. Xu J, Zhang C, He Y, Wu H, Wang Z, Song W, et al. Lymphatic endothelial cell-
640 secreted CXCL1 stimulates lymphangiogenesis and metastasis of gastric cancer.
641 International Journal of Cancer. 2012;130(4):787-797.
642 24. Schindelin J, Arganda-Carreras I, Frise E, Kaynig V, Longair M, Pietzsch T, et al.
643 Fiji: an open-source platform for biological-image analysis. Nature Methods.
644 2012;9:676-682.
645 25. Vierra A, Garret J. Understanding Interobserver Agreement: The Kappa Statistic.
646 Research Series. 2005;37(5).
647 26. Metsalu T, Vilo J. ClustVis: a web tool for visualizing clustering of multivariate data
648 using Principal Component Analysis and heatmap. Nucleic Acids Research.
649 2015;43(W1):W566-W570.
650 27. Vlachos I.S, Hatzigeorgiou AG. DIANA-miRPath v3. 0: deciphering microRNA
651 function with experimental support. Nucleic acids research. 2015;43:W460–W466.

652 28. Bhattacharya R, Nicoloso M, Arvizo R, Wang E, Cortez A, Rossi S, et al. MiR-15a
653 and MiR-16 Control Bmi-1 Expression in Ovarian Cancer. Cancer Research.
654 2009;69(23):9090–9095.
655 29. Petrillo M, Zannoni GF, Beltrame L, Martinelli E, DiFeo A, Paracchini L, et al.
656 Identification of high-grade serous ovarian cancer miRNA species associated with
657 survival and drug response in patients receiving neoadjuvant chemotherapy: a
658 retrospective longitudinal analysis using matched tumor biopsies. Annals of
659 Oncology. 2016;27(4):625-634.
660 30. Sorrentino A, Liu CG, Addario A, Peschle C, Scambia G, Ferlini C. Role of
661 microRNAs in drug-resistant ovarian cancer cells. Gynecologic Oncology.
662 2008;111(3):478 - 486.
663 31. Boyerinas B, Park SM, Hau A, Murmann AE, Peter ME. The role of let-7 in cell
664 differentiation and cancer. MicroRNA. 2012;1(1):34-39.
665 32. Cai J, Yang C, Yang Q, Ding H, Jia J, Guo J, et al. Deregulation of let-7e in epithelial
666 ovarian cancer promotes the development of resistance to cisplatin. Oncogenesis.
667 2013;2:e75
668 33. Liu N, Zhou C, Zhao J, Chen Y. Reversal of Paclitaxel Resistance in Epithelial
669 Ovarian Carcinoma Cells by a MUC1 Aptamer-let-7i Chimera. Cancer Investigation.
670 2012;30(8):577-582.
671 34. Gérard C, Lemaigre F, Gonze D. Modeling the Dynamics of Let-7-Coupled Gene
672 Regulatory Networks Linking Cell Proliferation to Malignant Transformation.
673 Frontiers in Physiology. 2019;10:848.

674 35. Meng F, Henson R, Wehbe-Janek H, Smith H, Ueno Y, Patel T. The MicroRNA let-
675 7a Modulates Interleukin-6-dependent STAT-3 Survival Signaling in Malignant
676 Human Cholangiocytes. Journal of Biological Chemistry. 2007;282(11):8256-8264.
677 35. Kumar M, Ahmad T, Sharma A, Mabalirajan U, Kulshreshtha A, Agrawal A, Ghosh
678 B. Let-7 microRNA-mediated regulation of IL-13 and allergic airway inflammation.
679 Journal of Allergy and Clinical Immunology. 2011;128(5):1077–1085.e10.
680 36. Choudhury S, Li Y. miR-21 and let-7 in the Ras and NF-IκβPathways. MicroRNA.
681 2012;1(1):65-69.
682 37. Cromer WE, Zawieja SD, Tharakan B, Childs EW, Newell MK, Zawieja DC. The
683 effects of inflammatory cytokines on lymphatic endothelial barrier function.
684 Angiogenesis. 2014;17(2):395–406.
685 38. Aldrich MB, Sevick-Muraca EM. Cytokines are systemic effectors of lymphatic
686 function in acute inflammation. Cytokine. 2013;64(1):362–369.
687 39. Chen W, Tang Z, Sun Y, Zhang Y, Wang X, Shen Z, et al. miRNA expression profile
688 in primary gastric cancers and paired lymph node metastases indicates that miR-10a
689 plays a role in metastasis from primary gastric cancer to lymph nodes. Experimental
690 and Therapeutic Medicine. 2012;3(2):351-356.
691 40. Sun CY, She XM, Qin Y, Chu ZB, Chen L, Ai LS, et al. miR-15a and miR-16 affect
692 the angiogenesis of multiple myeloma by targeting VEGF. Carcinogenesis. 2012;34.
693 41. Metsalu T, Vilo J. MicroRNA miR-93-5p regulates expression of IL-8 and VEGF in
694 neuroblastoma SK-N-AS cells.. Oncol Rep. 2016;35(5):2866-72.
695 42. Tzeng HE, Chang AC, Tsai CH, Wang SW, Tang CH. Basic fibroblast growth factor
696 promotes VEGF-C-dependent lymphangiogenesis via inhibition of miR-381 in human
697 chondrosarcoma cells. Oncotarget. 2016;7(25):38566–38578.

698 43. Yang G, Xiong G, Cao Z, Zheng S, You L, Zhang T, et al. miR-497 expression,
699 function and clinical application in cancer. Oncotarget. 2016;7(34):55900–55911.
700 45. Giacca M, Zacchigna S. VEGF gene therapy: therapeutic angiogenesis in the clinic
701 and beyond. Gene Therapy. 2012;19:622-629.
702 46. Kazenwadel J, Michael MZ, Harvey NL. Prox1 expression is negatively regulated by
703 miR-181 in endothelial cells. Blood. 2010;116(13):2395–2401.
704 47. Johnson NC, Dillard ME, Baluk P, McDonald DM, Harvey NL, Frase SL. Lymphatic
705 endothelial cell identity is reversible and its maintenance requires Prox1 activity.
706 Genes & Development. 2008;22(23):3282– 3291.
707 48. Reitsma S, Slaaf DW, Vink H, Zandvoort MAMJ, Egbrink MGA. The endothelial
708 glycocalyx: composition, functions, and visualization. European journal of
709 physiology. 2007;454(3):345–359.
710 49. Zolla V, Nizamutdinova IT, Scharf B, Clement CC, Maejima D, Akl T, et al. Aging-
711 related anatomical and biochemical changes in lymphatic collectors impair lymph
712 transport, fluid homeostasis, and pathogen clearance. Aging cell. 2015;14(4):582–
713 594.
714 50. Chakraborty S, Zawieja SD, Wang W, Lee Y, Wang YJ, von der Weid P, et al.
715 Lipopolysaccharide modulates neutrophil recruitment and macrophage polarization on
716 lymphatic vessels and impairs lymphatic function in rat mesentery. American journal
717 of physiology. Heart and circulatory physiology. 2015;309(12):H2042–H2057.
718

Supporting Information

S1 File. Supplementary information regarding building supervised classification algorithms. The techniques and assumptions when building classification algorithms and assessing the impact of individual miRNA.

S1 Table. Additional clinical data (patient age and surgery type).

S1 Fig. Experimental design for LV miRNA analysis from sample collection to analysis. Each vessel dissected from one sample is divided into 2 and processed for IHC and miRNA expression analysis.

S2 Table. Differential expression of miRNA between LVs from patients that relapsed within 13.2±6 months. Listed are miRNA that showed a fold-change ±1.8 and/ or a significant difference between groups (t-test $p>0.05$)

S2 Fig. The KDE estimations of the distributions of inner groups for the individual miRNA expressed at statistically significant levels ($p<0.05$) between LVs with high inflammation and LVs with low inflammation.

S3 Fig. A. Partial component analysis showed that inflamed and non-inflamed samples show variance across Principle Component (PC) 2. Samples with most similar miRNA expression profile cluster together. Unit variance scaling was applied to rows; SVD with imputation was used to calculate principal components. Prediction ellipses are such that with probability 0.95, a new observation from the same group will fall inside the ellipse. N = 10 data points. A scree plot confirmed that PC1 & PC2 accounted for much of the variation (S4

744 Fig). Figures produced with ClustVis[1] B. The miRNA expression driving PC1 & 2
745 contributed to the greatest variation between sample groups with several miRNA identified as
746 differentially regulated when comparing inflamed or cancer-infiltrated LVs (bold =>±1.8,
747 *=p<0.05).
748
749 **S4 Fig. A Principle Component Analysis scree plot for all samples analysed to ensure**
750 **the two primary principle components accounted for much of the variation.** PCA figures
751 produced with ClustVis [26].
752
753 **S3 Table. Table of Classification analysis for various Supervised Classification**
754 **Algorithms.** The accuracy of the algorithm is shown, Cohen's Kappa of inner agreement
755 between predicted and actual values, the accuracy for inner groups and McNemar's test
756 significance of equality of predicted probability (inner accuracy) between groups for each
757 state.
758 **S4 Table. Significance values for the t-test between the inner distributions of High**
759 **Inflammation and Low Inflammation when equality of variances is assumed or not**
760 **assumed.** Levene's Test is the test for the equality of the variances between the groups.

761 **S5 Table. Classifier predictions on the experimental data (on Monte Carlo simulation**
762 **results) based on the expression of significantly dysregulated miRNA, on prediction of**
763 **the examined states (e.g. Inflam, Cancer etc).** Accuracy, Cohen's Kappa, Mc Nemar p-
764 value of equality of inner grouped probabilities and classification are reported for the
765 predicted classes. The expression of the most significantly differentially expressed miRNA
766 were added one by one, or in pairs if significance was equal, into the parameter set used to
767 build the classifiers. When only significantly differentially expressed miRNA in the inflamed
768 state (high and medium inflammation versus low) were used to build the classifier, the

769 accuracy of subsequent predictions increased by 20-40% compared to classifiers based on all
770 available miRNA expression (S3 Table). Similar improvements were found in the accuracy
771 of classifiers predicting relapse and LV cancer-infiltration (Tables 6 and 7).

772

773

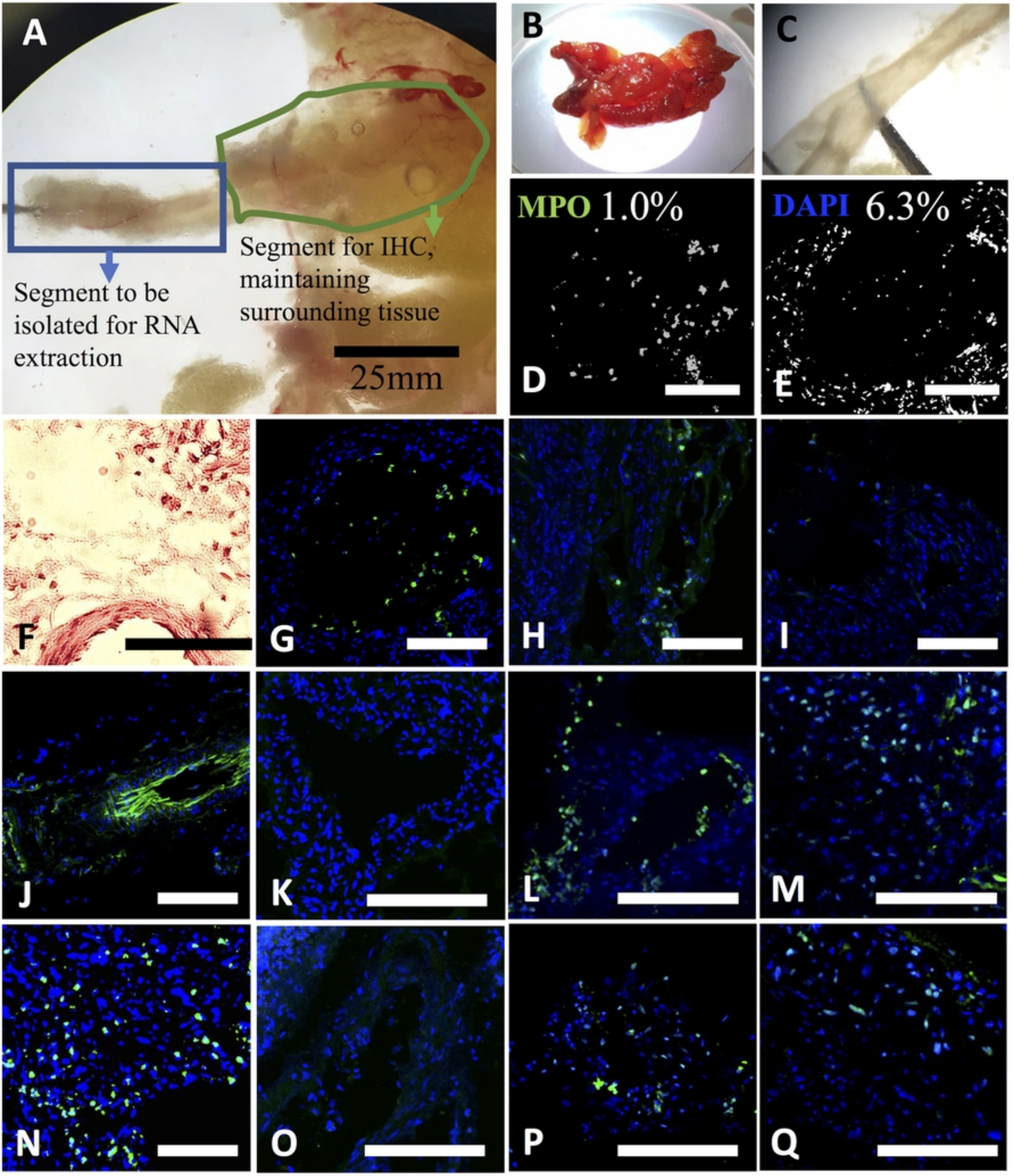
A
Segment to be isolated for RNA extraction
Segment for IHC, maintaining surrounding tissue
25mm
B
C
MPO 1.0%
D
DAPI 6.3%
E
F
G
H
I
J
K
L
M
N
O
P
Q

Figure 1

A

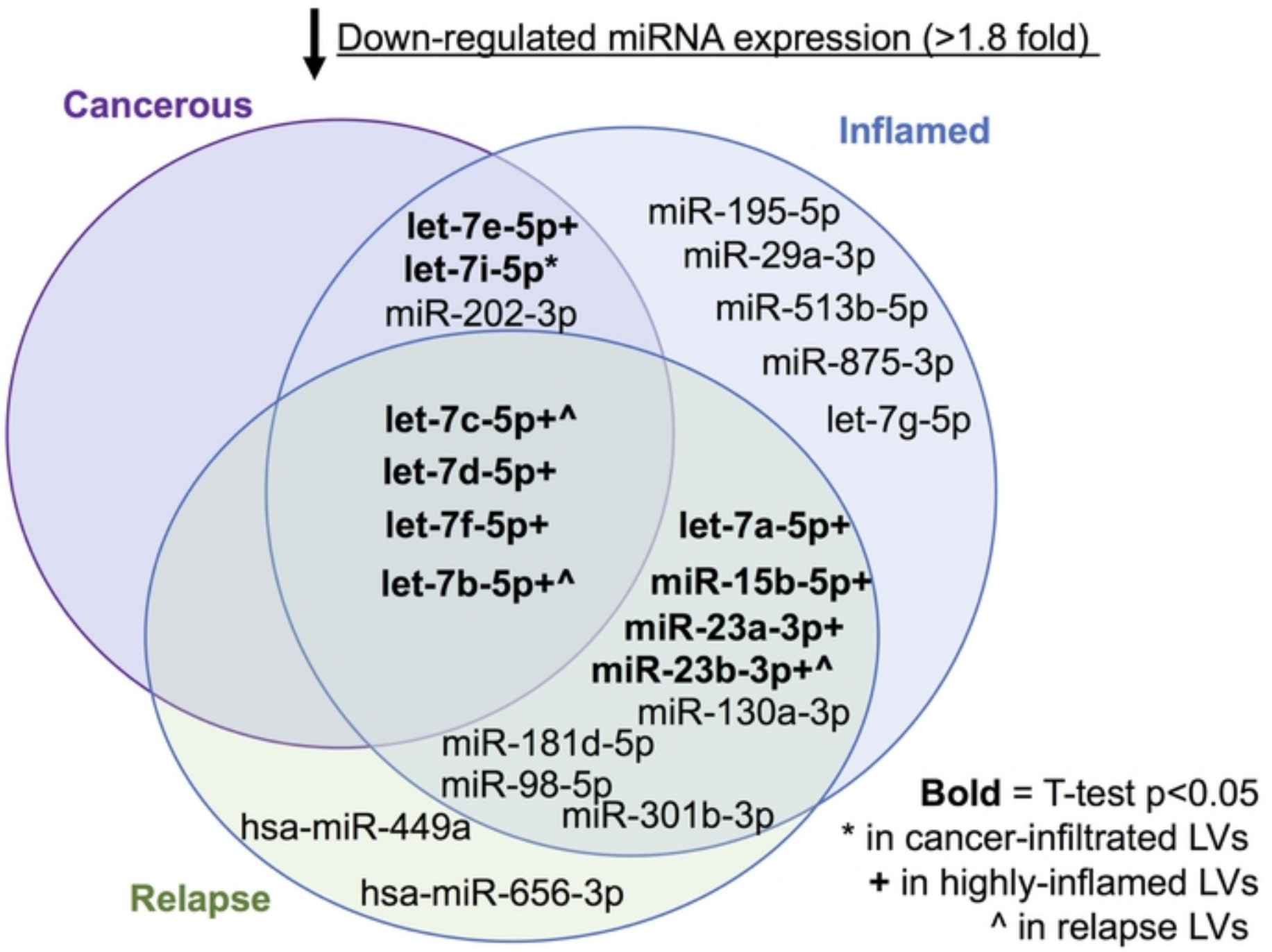
Down-regulated miRNA expression (>1.8 fold)
Cancerous
Inflamed
Relapse
let-7e-5p+
let-7i-5p*
miR-202-3p
miR-195-5p
miR-29a-3p
miR-513b-5p
miR-875-3p
let-7g-5p
let-7c-5p+^
let-7d-5p+
let-7f-5p+
let-7b-5p+^
let-7a-5p+
miR-15b-5p+
miR-23a-3p+
miR-23b-3p+^
miR-130a-3p
miR-181d-5p
miR-98-5p
miR-301b-3p
hsa-miR-449a
hsa-miR-656-3p
Bold = T-test p<0.05
* in cancer-infiltrated LVs
+ in highly-inflamed LVs
^ in relapse LVs

B

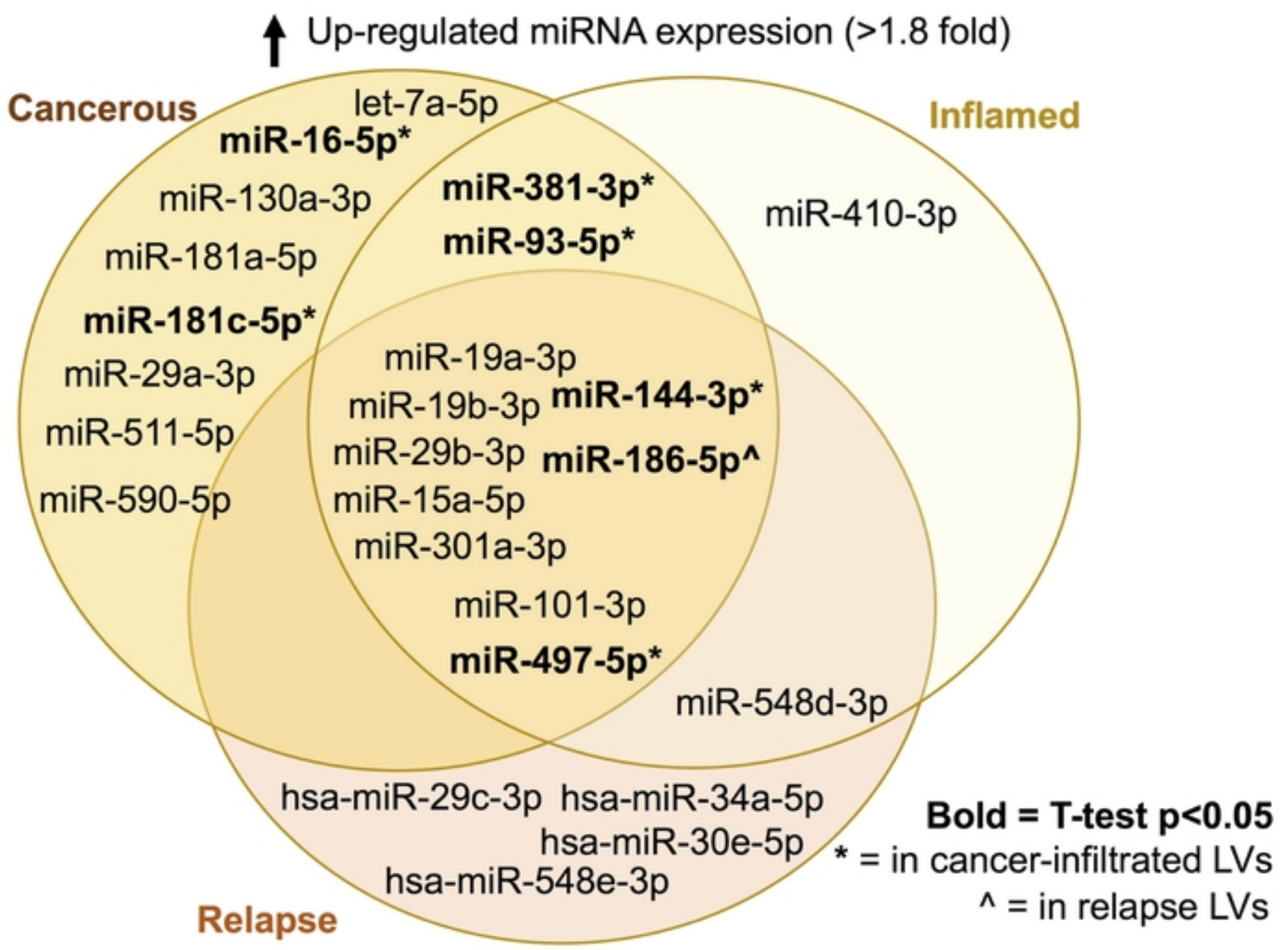
Up-regulated miRNA expression (>1.8 fold)
Cancerous
Inflamed
Relapse
let-7a-5p
miR-16-5p*
miR-130a-3p
miR-181a-5p
miR-181c-5p*
miR-29a-3p
miR-511-5p
miR-590-5p
miR-381-3p*
miR-93-5p*
miR-410-3p
miR-19a-3p
miR-19b-3p
miR-144-3p*
miR-29b-3p
miR-186-5p^
miR-15a-5p
miR-301a-3p
miR-101-3p
miR-497-5p*
miR-548d-3p
hsa-miR-29c-3p
hsa-miR-34a-5p
hsa-miR-30e-5p
hsa-miR-548e-3p
Bold = T-test p<0.05
* = in cancer-infiltrated LVs
^ = in relapse LVs

Figure 2